

Investigating the Polarization Tensor to Describe and Identify Metallic Objects

Taufiq K. A. Khairuddin, Paul D. Ledger and William R. B. Lionheart

Abstract—This paper presents a few properties of the polarization tensor for conducting and magnetic objects to describe and classify the objects. In order to achieve this, the polarization tensor of the objects are numerically determined by the previous *hp*-FEM method. We then focus on the polarization tensor for magnetic but non-conducting objects. After that, the polarization tensor for translated and rotated objects are discussed. Finally, this paper also highlights the polarization tensor for a few threat and non-threat objects which might appear in metal detection for security screening and landmine clearance.

Index Terms—metal detectors, land mine detection, eddy currents, *hp*-FEM method, matrices.

I. INTRODUCTION

IN the eddy current approximation to Maxwell's equation, Ammari et al. [1] derived an asymptotic formula that represented the perturbation of the magnetic fields due to the presence of an isolated conducting object. Two polarization tensors were then introduced from the formula, namely the conductivity polarization tensor (CPT) and the magnetic polarization tensor (MPT). They also designed a statistical algorithm to locate a spherical target based on induction data derived from eddy currents by using the CPT in [1] and extended it for an arbitrary target in [2].

Furthermore, based on the foundation given in [1], Ledger and Lionheart [3] further investigated the MPT and CPT to describe conducting and magnetic objects. The reduction in the number of independent coefficients for the CPT and MPT for objects with rotational and mirror symmetries were also highlighted. They also applied tensor operations to introduce a new polarization tensor by combining MPT and CPT.

In the engineering literatures, Marsh et al. [4], [5] reconstructed the magnetic polarizability tensor of several detected objects by making measurements of the fields generated by the metal detector in order to describe the location, dimension, orientation and material properties of an object for security screening. Similarly, Dekdouk et al. [6] conducted experiments to estimate the magnetic polarizability tensor of landmines to increase the chance of identifying them in a contaminated environmental field by using metal detector. It is shown in [3] that the magnetic polarizability tensor in [4], [5], [6] is the same as the rank 2 polarization tensor of [3] that combines both CPT and MPT.

In this study, the polarization tensor for a few objects are numerically computed according to the formula and method presented in [3].

Manuscript received March 13, 2015; revised April 9, 2015. This work was supported by the Ministry of Education of Malaysia and EPSRC under the grants EP/KO39865/1.

T. Khairuddin is with the School of Mathematics, The University of Manchester, UK and Department of Mathematical Sciences, Universiti Teknologi Malaysia, Johor Bharu, Malaysia. e-mail: (taufiq@utm.my).

P. Ledger is with the College of Engineering, Swansea University and W. Lionheart is with the School of Mathematics, The University of Manchester.

II. MATHEMATICAL FORMULATION OF THE POLARIZATION TENSOR

The mathematical formulation of the polarization tensor is discussed now by considering first the eddy current model presented in [3]. Following Ammari et al. [1], we assume the presence of an object in the form $B_\alpha = z + \alpha B$ where B is a unit object centered at the origin, α denotes a scaling for B and z denotes a translation vector. Introduce

$$\mu_\alpha = \begin{cases} \mu_* & \text{in } B_\alpha \\ \mu_0 & \text{in } \mathbb{R}^3 \setminus B_\alpha \end{cases}, \sigma_\alpha = \begin{cases} \sigma_* & \text{in } B_\alpha \\ 0 & \text{in } \mathbb{R}^3 \setminus B_\alpha \end{cases} \quad (1)$$

where μ_0 denotes the permeability of free space while both μ_* and σ_* denote the permeability and conductivity of the inclusion B_α . In this case, μ_* and σ_* are just constants and we drop the subscript $*$ when considering B later on. Moreover, the conductivity contrast between the object and the background is assumed to be sufficiently high that the background can be approximated by a zero conductivity.

Let E_α and H_α be the time harmonic eddy current fields (electric and magnetic) in the presence of conducting object B_α that result from a current source J_0 located outside B_α . Suppose that $\nabla \cdot J_0 = 0$ in \mathbb{R}^3 . Both fields E_α and H_α satisfy the eddy current equations

$$\nabla \times E_\alpha = i\omega\mu_\alpha H_\alpha \text{ in } \mathbb{R}^3, \quad (2)$$

$$\nabla \times H_\alpha = \sigma_\alpha E_\alpha + J_0 \text{ in } \mathbb{R}^3, \quad (3)$$

$$E_\alpha(x) = O(|x|^{-1}), H_\alpha(x) = O(|x|^{-1}) \text{ as } |x| \rightarrow \infty \quad (4)$$

where i is the standard imaginary unit and ω is a fixed angular frequency of the current source. The depth of penetration of the magnetic field in the conducting object is described by its skin depth, $s = \sqrt{2/(\omega\mu_0\sigma_*)}$. On the other hand, without the object B_α , the fields E_0 and H_0 that result from the time varying current source satisfy

$$\nabla \times E_0 = i\omega\mu_0 H_0 \text{ in } \mathbb{R}^3, \quad (5)$$

$$\nabla \times H_0 = J_0 \text{ in } \mathbb{R}^3, \quad (6)$$

$$E_0(x) = O(|x|^{-1}), H_0(x) = O(|x|^{-1}) \text{ as } |x| \rightarrow \infty. \quad (7)$$

By introducing $\nu = 2\alpha^2/s^2$, the related asymptotic formula for the above model that describes the perturbation in the magnetic field at a position x , away from z , due to the presence of B_α when $\nu = O(1)$ and $(\mu_*/\mu_0) = O(1)$ as $\alpha \rightarrow 0$ is given by Ammari et al. [1] in the form

$$\begin{aligned} (H_\alpha - H_0)(x) = & -\frac{i\nu\alpha^3}{2} \sum_{i=1}^3 H_0(z)_i \left(\int_B D_x^2 G(x, z) \xi \times \right. \\ & \left. (\theta_i + \hat{e}_i \times \xi) d\xi \right) + \alpha^3 \left(1 - \frac{\mu_0}{\mu_*} \right) \left(\sum_{i=1}^3 H_0(z)_i D_x^2 G(x, z) \right. \\ & \left. \int_B (\hat{e}_i + \frac{1}{2} \nabla \times \theta_i) d\xi \right) + R(x) \end{aligned} \quad (8)$$

where ξ is measured from the center of B . Here, $G(\mathbf{x}, \mathbf{z}) = (4\pi|\mathbf{x} - \mathbf{z}|)^{-1}$ is the free space Laplace Green's function and $\mathbf{R}(\mathbf{x}) = O(\alpha^4)$ is a small remainder term. Furthermore, for $i = 1, 2, 3$, \hat{e}_i is a unit vector for the i -th Cartesian coordinate direction, $\mathbf{H}_0(\mathbf{z})_i$ denotes the i -th element of $\mathbf{H}_0(\mathbf{z})_i$ and θ_i is the solution to the transmission problem

$$\begin{cases} \nabla_{\xi} \times \mu^{-1} \nabla_{\xi} \times \theta_i & \text{in } B \cup B^c, \\ -i\omega\sigma\alpha^2\theta_i = i\omega\sigma\alpha^2\hat{e}_i \times \xi & \\ \nabla_{\xi} \cdot \theta_i = 0 & \text{in } B^c, \\ [\theta_i \times \hat{n}]_{\Gamma} = 0 & \text{on } \Gamma, \\ [\mu^{-1} \nabla_{\xi} \times \theta_i \times \hat{n}]_{\Gamma} = -2[\mu^{-1}]_{\Gamma} \hat{e}_i \times \hat{n} & \text{on } \Gamma, \\ \theta_i(\xi) = O(|\xi|^{-1}) & \text{as } |\xi| \rightarrow \infty \end{cases} \quad (9)$$

where \hat{n} is the outward normal vector to Γ , the boundary of B . Based on (8), two polarization tensors are introduced by [1] namely the *conductivity polarization tensor* (CPT) and the *magnetic (permeability) polarization tensor* (MPT).

Using this framework, Ledger and Lionheart [3] have applied tensor operations to combine both CPT and MPT as well as reformulate (8) in the alternative form

$$(\mathbf{H}_{\alpha} - \mathbf{H}_0)(\mathbf{x}) = \mathbf{D}_x^2 G(\mathbf{x}, \mathbf{z}) M \mathbf{H}_0(\mathbf{z}) + \mathbf{R}(\mathbf{x}) \quad (10)$$

where M is the new polarization tensor for a conducting and magnetic inclusion B . In their study [3], M is expressed either as rank 4 or rank 2 tensor. The *hp*-finite element method presented in [7] is also used in [3] to numerically compute M as both rank 4 and rank 2 tensors. For the purpose of this study, the same M as the rank 2 tensor is considered where our main motivation for choosing this is because it agrees with the engineering prediction about the polarization tensor for metal detector [3]. The rank 2 tensor M is given by [3] as

$$M = N - C \quad (11)$$

where the coefficients of N and C are

$$\alpha^3 \left(1 - \frac{\mu_0}{\mu_*} \right) \int_B \left(\hat{e}_l \cdot \hat{e}_i + \frac{1}{2} \hat{e}_l \cdot \nabla \times \theta_i \right) d\xi \quad (12)$$

and

$$\left(-\frac{i\nu\alpha^3}{4} \right) \hat{e}_l \cdot \int_B \xi \times (\theta_i + \hat{e}_i \times \xi) d\xi \quad (13)$$

for $l = 1, 2, 3$.

III. METHODOLOGY

We now state several properties of the rank 2 tensor M . The coefficients of M can be expressed as 3×3 matrix and it is proven in [3] that M is complex symmetric so both real and complex parts of M have three real eigenvalues. In their studies, [3] also explain that $M = N$ for a magnetic non-conducting object B_{α} . Moreover, N here reduces to the first order Generalized Polarization Tensor (GPT) of [8] when B_{α} is simply connected and M can now be determined by solving boundary integral equations, which is given in [8] where the parameter k is the contrast μ_*/μ_0 (or the relative permeability of B_{α}). In this case, an analytical formula of M for an ellipsoid is also given.

Furthermore, M for an object B_{α} depends on the geometry, orientation and material of the object as given in (12) and (13). It also depends on the size but not on the position

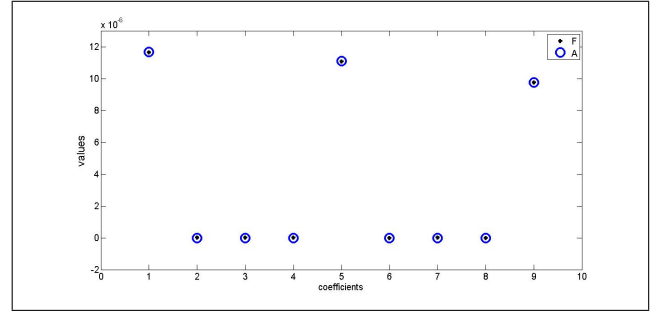


Fig. 1. A comparison between the coefficients of M for a magnetic but non-conducting ellipsoid as obtained by *hp*-FEM method (F) and the analytical solution (A)

of B_{α} . In addition, if the object B_{α} is rotated and becomes B'_{α} , it can be shown by following [2] and [8] that M for B'_{α} denoted by $M_{B'}$ satisfies the following relation

$$M_{B'} = \mathbf{R} M_B \mathbf{R}^T \quad (14)$$

where M_B is M for the original B_{α} , \mathbf{R} is the appropriate rotation matrix and \mathbf{R}^T is the transpose of \mathbf{R} .

In this study, the *hp*-FEM method described in [3] is also used here to numerically compute M for a series of known objects relevant to magnetic induction such as in metal detector. The object is firstly approximated by a tetrahedral mesh by using the *Netgen* mesh generator [9] (see pictures in Table IV and Table V for examples). The mesh can be generated either as linear or quadratic elements and both are supported in the method. However, if the object has curved boundary segments, quadratic elements must be selected for the mesh. Here, the convergence of M is achieved either by refining the size of the mesh in *Netgen* or by using higher degree polynomial of the edge element discretisation in the *hp*-FEM method.

IV. NUMERICAL RESULTS

The polarization tensor M for magnetic non-conducting objects is firstly computed and presented in this section where the coefficients (elements) of M in the first row are denoted starting from the first column by 1, 2 and 3 followed by 4, 5 and 6 for the second row, and 7, 8 and 9 for the third row. We then investigate M for a translated and rotated object. The polarization tensor M for a few threat and non-threat objects, which might appear in metal detection, are also considered.

A. M for Magnetic non Conducting Objects

Let B_{α} be the ellipsoid defined by $\frac{x^2}{a^2} + \frac{y^2}{b^2} + \frac{z^2}{c^2} = 1$ where $a = 0.3$, $b = 0.2$, $c = 0.1$ centimeters (cm) and suppose that B_{α} is non-conducting and its relative permeability is equal to 1.5. By using 11665 tetrahedral meshes and polynomials of degree three in the *hp*-FEM method, an agreement of the computed coefficients of M for B_{α} to the analytical solution [8] is obtained. Figure 1 compares every coefficient of M for B_{α} based on analytical solution given in [8] with the same coefficients of M computed by the *hp*-FEM method.

On the other hand, Figure 2 shows a comparison of the coefficients of M for a non-conducting toroidal object with relative permeability 500 computed based on boundary integral formula of the first order GPT in [8] and also by

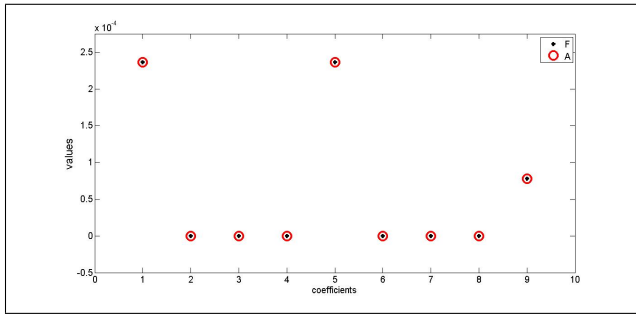


Fig. 2. A comparison between the coefficients of M for a magnetic but non-conducting torus as obtained by hp -FEM method (F) and the boundary integral formulation of the first order GPT in BEM++ (A)

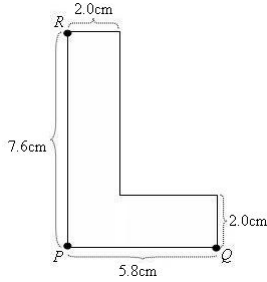


Fig. 3. The base of a L -shaped object

hp -FEM method. The diameter and height of the object are 0.2 and 0.1 cm, respectively, and the object has a cylindrical hole with diameter and height both approximately equal to 0.1 cm. Here, the convergence of M in the hp -FEM method is achieved by approximating the object by 27919 tetrahedral meshes and uniformly increasing the degree of polynomial until order three. On the other hand, the boundary integral formula in [8] is numerically approximated by the software called as BEM++ [10] which converges with 16174 surface elements.

B. M for a Translated and Rotated Object

In order to demonstrate the effect on the coefficients of the polarization tensor M under translation and rotation, we consider B_α as a three-dimensional L -shaped object (dimensions of the object are in cm). Here, the base of the object if viewed in two dimensions, is shown in Figure 3. Three points P , Q and R are also chosen for references when translating or rotating the object.

We now assign the base to be above the xy -plane and for any point, $p \in B_\alpha$ where (x_p, y_p, z_p) is the coordinate of p in the three dimensional Cartesian coordinate system, $x_p, y_p, z_p \geq 0$. We also let the height of the object to be equal to 1.5 so that $0 \leq z_p \leq 1.5$. In this case, P, Q and R are firstly set to be $(0,0,0)$, $(5.8,0,0)$ and $(0,7.6,0)$ respectively. The object is approximated in *Netgen* by a linear mesh and assuming that the object is both conducting and magnetic ($\sigma_* = 4.5 \times 10^6$ S/m (Siemens per meter) and $\mu_* = 1.26 \times 10^{-4}$ NA $^{-2}$ (Newton per ampere 2)), the convergence of M for the object denoted by M_L is obtained in the hp -FEM method by uniformly increasing the degree of polynomial until order three with 57456 tetrahedra. The converged M_L

is written in the form $M_L = \mathcal{R} + \mathcal{J}i$ where

$$\mathcal{R} = 10^{-3} \times \begin{bmatrix} 0.2314 & -0.0818 & 0 \\ -0.0818 & 0.3530 & 0 \\ 0 & 0 & 0.0686 \end{bmatrix} \quad (15)$$

and

$$\mathcal{J} = 10^{-3} \times \begin{bmatrix} -0.0200 & 0.0168 & 0 \\ 0.0168 & -0.0400 & 0 \\ 0 & 0 & -0.0024 \end{bmatrix}. \quad (16)$$

1) M for a translated object: In order to investigate M for the L -shaped object under a few translations, every point p that lies in the original object will be translated by a translation coordinate $v = (v_x, v_y, v_z)$ such that every p for the translated object becomes $(x_p + v_x, y_p + v_y, z_p + v_z)$. A few v are considered, as listed in Table I, where the new P, Q, R as well as the new minimum and maximum values of z_p are given. Each translated object is then created in *Netgen* and approximated by a linear tetrahedral mesh. Using these approximations, M for the object at every new position denoted by $M_{L'}$ is recomputed with the hp -FEM method. By using the third order polynomial, each $M_{L'}$ converges on the mesh with N number of tetrahedra, where N is also included in Table I.

Each $M_{L'}$ is now compared with the original M_L where $D_{L'} = M_{L'} - M_L$ is firstly determined in the software *MATLAB*. Let $\tilde{D}_{L'}$ be a 9×1 column vector which contains all coefficients of $D_{L'}$. By using the function `roundn` in *MATLAB*, $\tilde{D}_{L'}$ is round to 5 and `roundn($\tilde{D}_{L'}$, -5)` and `roundn($\tilde{D}_{L'}$, -6)`, respectively. The function `any` is then applied to `roundn($\tilde{D}_{L'}$, -5)` and `roundn($\tilde{D}_{L'}$, -6)` to decide whether $\tilde{D}_{L'}$ is a zero column vector or not. The outputs for commands `any(roundn($\tilde{D}_{L'}$, -5))` and `any(roundn($\tilde{D}_{L'}$, -6))` in *MATLAB* are given as $(d, -5)$ and $(d, -6)$ in the last two columns of Table I.

2) M for a rotated object: The L -shaped object at the original position in the Cartesian plane is now rotated three times. Points P, Q and R after rotation as well as minimum and maximum value for z_p of point p lying in the object, are given in Table II. The polarization tensor M for each object at the new position after rotation is denoted by M_{Lr} and computed after that. Similarly, each rotated object is firstly approximated by a linear tetrahedral mesh in *Netgen*. The number of elements N , needed for each M_{Lr} to converge after is computed by using the third order polynomial in the hp -FEM method are then given in Table II.

Next, the polarization tensor M_L for the object at the original position is transformed three different times by using (14) according to each rotation performed to the object. The resulting transformed M_L is denoted by \tilde{M}_{Lr} for each rotation r . The rotation matrix \mathbf{R} used for each transformation is shown in Table III. Each \tilde{M}_{Lr} is then compared to M_{Lr} by following the same steps as in the translation case. $(d_r, -5)$ and $(d_r, -6)$ in Table III are the results from *MATLAB* that tell whether a 9×1 column vector where its elements are all coefficients of $\tilde{M}_{Lr} - M_{Lr}$ is a zero vector or not.

C. M for Threat and Non-threat Objects

A knife, a gun (dimension and material for the gun and the knife are based on that given in [11]) and a detonator

TABLE I
TRANSLATION OF THE L-SHAPED OBJECT

Translation, L'	v	P	Q	R	$z_p^{(min)}$	$z_p^{(max)}$	N	(d, j)	
								$j = -5$	$j = -6$
1	(2,2,2)	(2,2,2)	(7.8,2,2)	(2,9,6,2)	2	3.5	52993	0	1
2	(2,2,-2)	(2,2,-2)	(7.8,2,-2)	(2,9,6,-2)	-2	-0.5	55096	0	1
3	(-6,2,2)	(-6,2,2)	(-0.2,2,2)	(-6,9,6,2)	2	3.5	55871	0	1
4	(-6,2,-2)	(-6,2,-2)	(-0.2,2,-2)	(-6,9,6,-2)	-2	-0.5	54844	0	1
5	(2,-8,2)	(2,-8,2)	(7.8,-8,2)	(2,-0.4,2)	2	3.5	54242	0	1
6	(2,-8,-2)	(2,-8,-2)	(7.8,-8,-2)	(2,-0.4,-2)	-2	-0.5	51678	0	1
7	(-6,-8,2)	(-6,-8,2)	(-0.2,-8,2)	(-6,-0.4,2)	2	3.5	53723	0	1
8	(-6,-8,-2)	(-6,-8,-2)	(-0.2,-8,-2)	(-6,-0.4,-2)	-2	-0.5	51248	0	1
9	(-1,-1,-0.5)	(-1,-1,-0.5)	(4.8,-1,-0.5)	(-1,6.6,-0.5)	-0.5	1	54918	0	1

TABLE II
ROTATION OF THE L-SHAPED OBJECT (A)

Rotation, r	P	Q	R	$z_p^{(min)}$	$z_p^{(max)}$	N
90° around xy -plane	(0,0,0)	(0,-5.8,0)	(7.6,0,0)	0	1.5	41583
90° around xz -plane	(0,0,0)	(0,0,5.8)	(0,7.6,0)	0	5.8	58648
90° around yz -plane	(0,0,0)	(5.8,0,0)	(0,0,7.6)	0	7.6	42358

TABLE III
ROTATION OF THE L-SHAPED OBJECT (B)

Rotation, r	R	$(d_r, -5)$	$(d_r, -6)$
90° around z -axis	$\begin{bmatrix} 0 & -1 & 0 \\ 1 & 0 & 0 \\ 0 & 0 & 1 \end{bmatrix}$	0	0
90° around y -axis	$\begin{bmatrix} 0 & 0 & -1 \\ 0 & 1 & 0 \\ 1 & 0 & 0 \end{bmatrix}$	0	0
90° around x -axis	$\begin{bmatrix} 1 & 0 & 0 \\ 0 & 0 & -1 \\ 0 & 1 & 0 \end{bmatrix}$	0	0

analogue (DA) of type 72 AP-mine [6] are categorized as threat objects. On the other hand, the following non-threat objects are considered : 1 pound British coin [12], a ball bearing (diameter 0.9 cm) and a belt buckle (see [11] for example). After choosing suitable values of ω for a metal detector and setting μ_* (NA^{-2}) and σ_* (S/m) for each object according to its material, M for each object denoted by M_B is computed by hp -FEM method. During all computations, after every object is approximated by N tetrahedral elements (mesh for both knife and gun are linear while others are quadratic), every converged M_B is obtained when the degree of the polynomial is increased uniformly to the third order in the hp -FEM method. Table IV and Table V shows the number of elements, N needed by M_B for threat and non-threat object to converge.

In order to describe and identify each object, we first note that each M_B can be expressed as $M_B = \mathcal{R}_B + \mathcal{J}_B i$ where \mathcal{R}_B and \mathcal{J}_B are real symmetric 3×3 matrices containing all real and complex coefficients of M_B , respectively. Two real symmetric 3×3 matrices $M_{\mathcal{R}_B}$ and $M_{\mathcal{J}_B}$ are now introduced where elements of $M_{\mathcal{R}_B}$ are absolute value of elements

(coefficients) of \mathcal{R}_B while elements of $M_{\mathcal{J}_B}$ are absolute value of elements of \mathcal{J}_B . Let $\hat{e}_{M_{\mathcal{R}_B}}$ be a column vector containing all normalized eigenvalues of $M_{\mathcal{R}_B}$ such that $\hat{e}_{M_{\mathcal{R}_B}}$ contains every ratio of the eigenvalues of $M_{\mathcal{R}_B}$ to the largest eigenvalues of $M_{\mathcal{R}_B}$. On the other hand, let $\hat{e}_{M_{\mathcal{J}_B}}$ be a column vector containing every ratio of the eigenvalues of $M_{\mathcal{J}_B}$ to the largest eigenvalues of $M_{\mathcal{J}_B}$. We propose to use $\hat{e}_{M_{\mathcal{R}_B}}$ and $\hat{e}_{M_{\mathcal{J}_B}}$ instead of the original M_B for describing and identifying each object where $\hat{e}_{M_{\mathcal{R}_B}}$ and $\hat{e}_{M_{\mathcal{J}_B}}$ are also given in Table IV and Table V.

V. DISCUSSION AND CONCLUSION

This paper discusses an approach to describe conducting and magnetic metallic objects by using the polarization tensor, M . By considering a potential application in metal detection, mathematical formulation of the rank 2 M from the eddy current model which is based on [3] is reviewed. We also highlight several properties of M that are very useful to our purpose. During several studies conducted by engineers [4], [5], [6], polarization tensor for a few tested objects were reconstructed from metal detector measurements to describe

TABLE IV
THE NORMALIZED EIGENVALUES OF M FOR THREAT OBJECTS

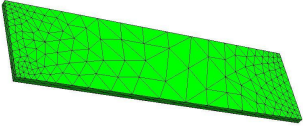
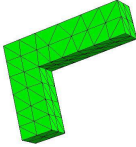
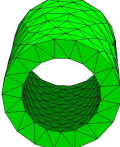
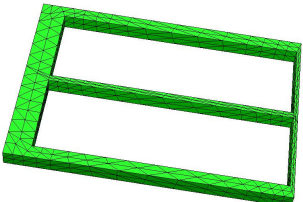
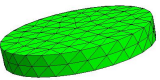
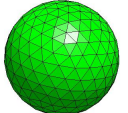
Object, B	Material	N	$\hat{e}_{M_{\mathcal{R}_B}}$	$\hat{e}_{M_{\mathcal{J}_B}}$
 Knife	stainless-steel $\mu_* = 1.26 \times 10^{-6} NA^{-2}$ $\sigma_* = 1.39 S/m$	13621	1	1
			0.9996	0.9355
			0.9957	0.0651
 Gun	type I steel $\mu_* = 1.26 \times 10^{-4} NA^{-2}$ $\sigma_* = 4.50 \times 10^6 S/m$	57456	1	1
			0.4826	0.2113
			0.1741	0.0480
 DA of 72 AP-mine	aluminium $\mu_* = 1.26 \times 10^{-6} NA^{-2}$ $\sigma_* = 3.50 \times 10^7 S/m$	17257	1	1
			0.3781	0.8578
			0.3781	0.8578

TABLE V
THE NORMALIZED EIGENVALUES OF M FOR NON-THREAT OBJECTS

Object	Material	N	$\hat{e}_{M_{\mathcal{R}_B}}$	$\hat{e}_{M_{\mathcal{J}_B}}$
 Belt Buckle	titanium $\mu_* = 1.26 \times 10^{-6} NA^{-2}$ $\sigma_* = 2.38 \times 10^6 S/m$	32640	1	1
			0.9995	0.0100
			0.4170	0.0069
 1 Pound Coin	nickel-brass $\mu_* = 1.26 \times 10^{-6} NA^{-2}$ $\sigma_* = 15.90 \times 10^6 S/m$	23930	1	1
			0.0083	0.0475
			0.0083	0.0475
 Ball Bearing	type II steel $\mu_* = 4.40 \times 10^{-4} NA^{-2}$ $\sigma_* = 4.65 \times 10^6 S/m$	6252	1	1
			1	1
			1	1

them. In contrast to their works, polarization tensor for a few specified objects are numerically computed by solving (9) and using (11) in this study.

In order to provide numerical examples for this study, M for magnetic but non conducting objects are firstly considered. Since M in this case reduces to the first order GPT of Ammari and Kang [8] for simply connected objects, the accuracy of the computed M for the object can then

be checked with the formula of GPT. An ellipsoid and a torus are chosen for this purpose where we consider a low permeability contrast for ellipsoid and a high permeability contrast for torus. The ellipsoid is chosen because there is a specified analytical formula for its first order GPT. On the other hand, the torus with the chosen permeability is a model of toroidal inductor, built by strong magnetic material, for example ferrite (nickel zinc). Figure 1 and Figure 2

show excellent agreement between M computed by the given formula through hp -FEM method and the first order GPT. It can be seen that M for both ellipsoid and torus here are diagonal matrices. In addition, the first diagonal and the second diagonal entries of M for the torus are equal.

Next, M for a translated and rotated object are examined. The three dimensional L -shaped object used here with the chosen μ_* and σ_* is actually the steel gun in Table IV. A real situation is actually considered as our main motivation for this investigation where a person might carry a gun with many possible orientations on any part of his body when passing a metal detector during security checking. For this purpose, we first compute M for the object at a chosen initial position by using the hp -FEM method, resulting to the real and imaginary coefficients (15) and (16). The results show that M is complex symmetric as predicted by the theory in [3] for a conducting and magnetic object.

The results after 9 translations have been performed to the object are shown in Table I where the first eight of L' move the object in each octant of the three dimensional space without including the origin. The last L' translates the object from its initial position and lies within the intersection of every octant in three dimensional space, which will include the origin. M of the object at the original (initial) position is then compared to M for the object after it has been translated, which is also computed by the hp -FEM method. The values $(d, -5)$ and $(d, -6)$ in Table I are tests done in *MATLAB* to decide whether $\tilde{D}_{L'}$ is a zero column vector or not after is rounded to 5 and 6 decimal places. If the value is 0 then $\tilde{D}_{L'}$ is a zero column vector while 1 indicates that $\tilde{D}_{L'}$ has at least one non-zero element. In this case, for each L' , $\tilde{D}_{L'}$ is a 9×1 zero column vector after is rounded to 5 decimal places which implies $D_{L'} = M_{L'} - M_L$ is a zero matrix of size 3 and hence, $M_{L'} = M_L$ for all L' at 5 decimal places or less, that is M of each translated object is the same as M of the object before translation. The results here consistent with our previous theory that M does not depend on the position of the object.

In addition, similar tests are performed in *MATLAB* to decide whether M of rotated objects computed by the hp -FEM method is similar to transforming M of the object at the original (initial) position according the same rotation. The results in Table II show that a column vector containing all coefficients of $\tilde{M}_{Lr} - M_{Lr}$ is a zero vector after is rounded to 5 and 6 decimal places. Consequently, at 6 decimal places or less, $\tilde{M}_{Lr} - M_{Lr}$ is a zero matrix of size 3 so $\tilde{M}_{Lr} = M_{Lr}$ for each r such that M of all rotated objects are similar to transforming M of the object at original position. These also give numerical evidences to suggest that M for the object at original position can be used directly to find M for the object after it is rotated, as given by (14). Therefore, it is then possible to identify an unknown object by reconstructing and comparing its M to any transformed M for a known object.

Finally, we also compute M for a few threat and non-threat objects in metal detection. A coin, a ball bearing of a toy (such as a yo-yo) and a belt buckle are non-threat objects during security check and coin also is a wanted object in treasure hunting by metal detector. Meanwhile, a gun and a knife are threat objects in security screening and a detonator analogue (DA) of type 72 AP-mine is the most important part in land mine detection. Here, the normalized eigenvalues

for real and imaginary parts of M are used to describe all objects. Based on Table IV and Table V, we can see that ball bearing has one distinct normalized eigenvalues for both real and imaginary parts of its M , coin and DA have two for each parts while others has three. Moreover, in contrast to other objects, DA and coin have the normalized eigenvalues of the imaginary parts to be either larger or equal to the normalized eigenvalues of the real part. This information is very useful to describe and classify the objects and can be further investigated. Our main aim after this will be to compare these results with the reconstructed polarization tensor and analyze them to hopefully improve metal detection in the future.

ACKNOWLEDGMENT

The authors were very grateful to Prof. Tony Peyton and Dr. Liam Marsh for their useful discussions on metal detection and to Prof. Habib Ammari for his helpful suggestions.

REFERENCES

- [1] H. Ammari, J. Chen, Z. Chen, J. Garnier and D. Volkov, "Target detection and characterization from electromagnetic induction data," *Journal de Mathématiques Pures et Appliquées*, **101**, 54-75, 2014.
- [2] H. Ammari, J. Chen, Z. Chen, D. Volkov and H. Wang, "Detection and classification from electromagnetic induction data," submitted.
- [3] P. D. Ledger and W. R. B. Lionheart, "Characterising the shape and material properties of hidden targets from magnetic induction data," submitted.
- [4] L. A. Marsh, C. Ktistis, A. Järvi, D. W. Armitage and A. J. Peyton, "Three-dimensional object location and inversion of the magnetic polarizability tensor at a single frequency using a walk-through metal detector," *Measurement Science and Technology*, **24**(4), 2013.
- [5] L. A. Marsh, C. Ktistis, A. Järvi, D. W. Armitage and A. J. Peyton, "Determination of the magnetic polarizability tensor and three dimensional object location for multiple objects using a walk-through metal detector," *Measurement Science and Technology*, **25**(5), 2014.
- [6] B. Dekdouk, L. A. Marsh, D. W. Armitage, and A. J. Peyton, "Estimating magnetic polarizability tensor of buried metallic targets for landmine clearance," *Springer Science and Business Media*, 425-432, LLC:2014.
- [7] P. D. Ledger and S. Zaglmayr, " hp -Finite element simulation of three-dimensional eddy current problems on multiply connected domains," *Computer Methods in Applied Mechanics and Engineering*, **199**, 49-52, 2010.
- [8] H. Ammari and H. Kang, *Polarization and Moment Tensors : with Applications to Inverse Problems and Effective Medium Theory*, *Applied Mathematical Sciences Series*, **162**, Springer-Verlag, New York, 2007.
- [9] J. Schöberl "NETGEN : An advancing front 2D/3D-mesh generator based on abstract rules," *Comput Visual Sci*, **1**, 41-52, 1997.
- [10] W. Śmigaj, S. Arridge, T. Betcke, J. Phillips and M. Schweiger, "Solving boundary integral problems with BEM++," to appear in *ACM Trans. Math. Software*.
- [11] Walk-Through Metal Detectors for Use in Concealed Weapon and Contraband Detection. <https://www.ncjrs.gov/pdffiles1/nij/193510.pdf>
- [12] http://en.wikipedia.org/wiki/One_pound_%28British_coin%29